Novel insights into the assembly and function of human nuclear-encoded cytochrome c oxidase subunits 4, 5a, 6a, 7a and 7b

Daniela Fornuskova, Lukas Stiburek, Laszlo Wenchich, Kamila Vinsova, Hana Hansikova, Jiri Zeman

Novel insights into the assembly and function of human nuclear-encoded cytochrome *c* oxidase subunits 4, 5a, 6a, 7a and 7b

Daniela Fornuskova, Lukas Stiburek, Laszlo Wenchich, Kamila Vinsova, Hana Hansikova, Jiri Zeman*

Department of Pediatrics, First Faculty of Medicine, Charles University in Prague, Czech Republic

Short (page heading) title:
Assembly and function of nuclear-encoded CcO subunits 4, 5a, 6a, 7a and 7b

**To whom correspondence should be addressed:*
Prof. Jiri Zeman, MD, PhD
Department of Pediatrics
Faculty of Medicine, Charles University in Prague
Ke Karlovu 2, Prague 2, 128 08, Czech Republic
Phone: +420-2-24967733
Fax: +420-2-24967099
Email: jzem@lf1.cuni.cz

Keywords
biogenesis, cytochrome *c* oxidase, assembly, respiratory supercomplexes, RNA interference

Abbreviations used: BN/SDS-PAGE, blue native/denaturing polyacrylamide gel electrophoresis; CcO, cytochrome *c* oxidase; DDM, n-dodecyl-β-D-maltoside; FCCP, p-trifluoromethoxophenylhydrazone; KD, knockdown; NS, control, non-silencing shRNA; RNAi, RNA interference; SQR, succinate:coenzyme Q_{10} reductase, complex II; TMPD, N,N,N',N'-tetramethyl-p-phenylenediamine dihydrochloride; UTR, untranslated region of mRNA.

Biochemical Journal Immediate Publication. Published on 22 Mar 2010 as manuscript BJ20091714

SYNOPSIS

Mammalian cytochrome *c* oxidase (CcO) is a hetero-oligomeric protein complex composed of 13 structural subunits encoded by both the mitochondrial and nuclear genomes. To study the role of nuclear-encoded CcO subunits in the assembly and function of the human complex, we used stable RNA interference of COX4, COX5A and COX6A1, as well as expression of epitope-tagged Cox6a, Cox7a and Cox7b, in human HEK293 cells. Knockdown of Cox4, Cox5a and Cox6a resulted in reduced CcO activity, diminished affinity of the residual enzyme for oxygen, decreased holoCcO and CcO dimer levels, increased accumulation of CcO subcomplexes and an altered pattern of respiratory supercomplexes. An analysis of the patterns of CcO subcomplexes found in both knockdown and overexpressing cells identified a novel CcO assembly intermediate, identified the entry points of three late-assembled subunits and directly demonstrated the essential character as well as the interdependence of the assembly of Cox4 and Cox5a. The ectopic expression of the heart/muscle-specific isoform of the Cox6 subunit (COX6A2) resulted in restoration of both CcO holoenzyme and activity in COX6A1 knockdown cells. This was in sharp contrast to the unaltered levels of COX6A2 mRNA in these cells, suggesting the existence of a fixed expression program. The normal amount and function of respiratory complex I in all of our CcO deficient knockdown cell lines suggest that unlike non-human CcO-deficient models, even relatively small amounts of CcO can maintain the normal biogenesis of this respiratory complex in cultured human cells.

INTRODUCTION

Cytochrome *c* oxidase (CcO), the terminal enzyme complex of the mitochondrial electron-transport chain couples the electron transfer from reduced cytochrome *c* to molecular oxygen with vectorial proton translocation across the inner membrane. The mammalian CcO complex is composed of 13 different polypeptide subunits, which are encoded by both the nuclear and mitochondrial genomes. Mitochondrially encoded Cox1 and Cox2 form the redox site involved in electron transfer. Electrons enter the CcO complex at the binuclear copper site (Cu_A) in the Cox2 subunit, which also mediates electrostatic binding of cytochrome *c* [1]. From Cu_A, electrons pass to other metal centers in the Cox1 subunit, first to heme *a* and then to a heterobimetallic heme a_3/Cu_B center [2]. Together with Cox3, mitochondrially encoded subunits constitute the evolutionarily conserved structural core of the enzyme. The remaining ten subunits, which are encoded by nuclear DNA, are associated with the surface of the complex core. These small polypeptides are required for the assembly and stability of the holoenzyme and are thought to function in the regulation of its activity [3-5]. Tissue-specific isoforms of subunits Cox4, Cox6a, Cox6b, Cox7a and Cox8 have been identified in mammals [6, 7]. Most CcO subunits have one or more transmembrane domains, with the exception of Cox5a and Cox5b, which are located at the matrix side, and Cox6b, which is associated with the surface of the complex in the intermembrane space [8].

Subunit Cox4 is the largest nuclear-encoded subunit of the complex. It was shown to be involved in the allosteric inhibition of CcO activity by ATP, which binds to the matrix portion of the subunit [9]. Isoforms 1 and 2 of Cox4 are encoded by two separate genes and are likely to differ with respect to ATP-induced inhibition of CcO activity [10]. In mammalian cells, the first step of CcO assembly is the membrane integration of Cox1, followed by the association of the Cox4.Cox5a heterodimer [11]. Thus, subunit Cox5a indirectly binds to subunit Cox1 via the matrix domain of subunit Cox4 and the extramembrane segment of Cox6c. Subunit Cox6a is involved in the stabilization of the dimeric state of CcO and may contribute to the formation of an interaction site for cytochrome *c* [8]. Liver-type subunit Cox6a (Cox6a1/Cox6aL) is found in all non-muscle tissues, whereas heart/muscle-type subunit Cox6a (Cox6a2/Cox6aH), which is encoded by a different gene, is expressed only in striated muscles [12]. Subunit Cox6a was shown to associate with the complex, together with subunits Cox7a or Cox7b, at a very late stage of CcO assembly [13].

In the present work, we generated HEK293 cell lines with stably (shRNA) downregulated levels of CcO subunits Cox4, Cox5a and Cox6a. We analyzed the steady-state levels of the CcO holoenzyme and the presence and composition of CcO subcomplexes. We directly demonstrate that depletion of each of the selected subunits results in decreased levels of CcO with a parallel accumulation of CcO subcomplexes and unassembled subunits. These changes were accompanied by a reduction in the activity of CcO and a decreased affinity of CcO for oxygen. The subunit composition of CcO subcomplexes in Cox6a-depleted cells, along with analyses of the ectopic expression of subunits Cox7a2 and Cox7b in these cells, provided novel insights into the late stages of human CcO assembly. Moreover, CcO deficiency in COX6A1 knockdown cells was complemented by ectopic expression of the Cox6a2 isoform. We further demonstrate that CcO deficiency in COX5A and COX6A knockdown cells affects the formation of respiratory supercomplexes containing the dimeric form of CcO.

EXPERIMENTAL

Plasmid construction

The nucleotide sequences of 33 different candidate miR-30-based shRNAs (shRNAmirs) targeted to *COX4I1*, *COX5A* and *COX6A1* mRNAs were designed with shRNA Retriever (http://katahdin.cshl.org:9331/homepage/siRNA/RNAi.cgi?type=shRNA), synthesized and cloned into the pCMV-GIN-ZEO plasmid as previously described [14]. A pCMV-GIN-ZEO derivative that expresses negative control (non-silencing) shRNAmir was obtained from Open Biosystems. The coding sequences of COX7A2 (BC100852; IMAGE ID: 40002220) and COX7B (BC018386; IMAGE ID: 3861730) were amplified from the respective full-length cDNA clones (ImaGenes, Berlin, Germany), fused to the C-terminal FLAG epitope and cloned (*Eco*RI/*Not*I) into the modified pmaxFP-Red-N plasmid (Amaxa, Cologne, Germany). The fidelity of all constructs was confirmed by automated DNA sequencing. Plasmids pReceiver-M02 (EX-C0224) and pReceiver-M13 (EX-C0224) (GeneCopoeia, Germantown, MA) were used to express COX6A2 and COX6A2-FLAG, respectively.

Cell culture and transfection

Human embryonic kidney cells (HEK293, CRL-1573) were obtained from ATCC (Rockville, MD) and grown at 37 °C in 5% (v/v) CO_2 atmosphere in high-glucose Dulbecco's Modified Eagle's Medium (PAA, Pasching, Austria) supplemented with 10% (v/v) fetal bovine serum Gold (PAA). Cell lines stably expressing shRNAmir were prepared using the Nucleofector™ device (Amaxa) essentially as described previously [14]. The transient expression of selected CcO subunits in HEK293 cells was accomplished using the Express-In Transfection Reagent (Open Biosystems).

Reverse transcription and qRT-PCR

Total RNA was isolated from HEK293 cells using TriReagent solution (MRC, Cincinnati, OH). First strand complementary DNA (cDNA) was synthesized from 4 μg of total RNA with the use of Superscript III Reverse Transcriptase (Invitrogen, Carlsbad, CA) and Oligo-dT primers (Promega, Madison, WI) (RT^+). Preamplification and relative quantification was performed according to the manufacturer's instructions (Applied Biosystems, Foster City, CA). Ten preamplification cycles were run with 12.5 μl of cDNA and a 0.05x pooled mix of eight TaqMan Gene Expression Assays (Hs00971639_m1, COX4I1; Hs00261747_m1, COX4I2; Hs01924685_g1, COX6A1; Hs00193226_g1, COX6A2; Hs00427620_m1, TBP; Hs00173304_m1, PPARGC1A; Hs00188166_m1, SDHA; Hs01082775_m1, TFAM). Relative quantification was performed in duplicates twice on the 7300 Real Time PCR System (Applied Biosystems). The transcript levels of all mRNAs were normalized to the level of *TBP* (TATA box binding protein) mRNA. Because the amplification efficiency of the reference and target genes was the same, the comparative ΔΔCt method was used for relative quantification.

Immunoblot analysis

Protein sample preparation and signal acquisition for SDS, BN (Blue-Native) and BN/SDS-PAGE immunoblot analysis were performed essentially as described in [11, 14]. The immunoblots were developed with SuperSignal West Femto Maximum Sensitivity Substrate (Thermo Scientific, Waltham, MA). For analysis of respiratory supercomplexes by BN/SDS-PAGE and BN/BN-PAGE, isolated mitochondria were extracted using digitonin (detergent/protein ratio of 6 g/g). Primary detection of BN/SDS-PAGE and BN/BN-PAGE immunoblots was performed with mouse monoclonal antibodies (Mitosciences, Eugene, OR)

raised against the complex I subunit NDUFB6, complex III subunit Core1 and complex IV subunit COX1. The first dimension gel strips for BN/BN-PAGE immunodetection were soaked in cathode buffer containing 0.1% n-dodecyl-β-D-maltoside (DDM) for 15 min and then in cathode buffer containing 0.02% DDM for another 15 min. The second dimension of BN-PAGE separation was performed in the presence of 0.02% DDM as described in [15].

Spectrophotometric assays

The activities of respiratory chain complexes were measured spectrophotometrically with a UV-2401PC instrument (Shimadzu, Kyoto, Japan). Rotenone-sensitive complex I activity (NADH: ubiquinone oxidoreductase) was measured incubating 45 µg of mitochondrial protein in 1 ml of assay medium (50 mM TRIS, pH 8.1, 2.5 mg/ml BSA, 50 µM decylubiquinone, 0.3 mM KCN, 0.1 mM NADH without and with 3 µM rotenone). The decrease in absorbance at 340 nm due to the NADH oxidation was followed. Complex II activity (succinate - 2,6-dichloroindophenol oxidoreductase) was measured by incubating 20 µg of mitochondrial extract in 1 ml of assay medium (10 mM potassium phosphate pH 7.8, 2 mM EDTA, 1 mg/ml BSA, 0.3 mM KCN, 10 mM succinate, 3 µM rotenone, 0.2 mM ATP, 80 µM 2,6-dichloroindophenol, 1 µM Antimycin, 50 µM decylubiquinone). The decrease in absorbance at 600 nm due to the oxidation of 2,6-dichloroindophenol was followed. CcO activity (cytochrome *c* oxidase) was measured by incubating 15-18 µg of mitochondrial protein in 1 ml of assay medium (40 mM potassium phosphate, pH 7.0; 1 mg/ml BSA; 25 µM reduced cytochrome *c*; 2.5 mM n-dodecyl-β-D-maltoside) and the oxidation of cytochrome *c* (II) at 550 nm was followed. All assays were performed at 37^0C. The total protein was determined by the method of Lowry[16].

High-resolution respirometry and oxygen kinetics

Oxygen consumption measurements were performed as described previously [14], except that the cells were permeabilized with 50-75 µg/ml digitonin and 0.5 µM carbonylcyanide p-trifluoromethoxophenylhydrazone (FCCP) was used to uncouple and maximally stimulate respiration. The P_{50} value was measured in the presence of 0.5 µM FCCP and 10 mM succinate essentially as described in [17]. All measurements were performed independently three to six times for each cell line.

RESULTS

COX4I1 and COX6A1 isoforms account for the majority of COX4 and COX6A transcripts expressed in HEK293 cells under normal conditions

Because two tissue-specific isoforms of subunits COX4 and COX6A were described in humans, we measured the levels of *COX4I1*, *COX4I2, COX6A1* and *COX6A2* mRNAs in HEK293 cells. To quantify both isoforms using qRT-PCR, preamplification of the cDNA was necessary. The transcript levels of all mRNAs were normalized to the level of *TBP* mRNA. The relative normalized level of *COX4I1* mRNA was found to be ~2 x 10^5 times higher than *COX4I2*, whereas the relative normalized level of *COX6A1* mRNA was ~5 x 10^6 times higher than *COX6A2* (Fig. 1A). This finding suggests that the vast majority of Cox4 and Cox6a expressed and assembled within the CcO complex in HEK293 cells are represented by Cox4i1 and Cox6a1 tissue isoforms.

Subunits Cox4, Cox5a and Cox6a are depleted in HEK293 cells by the stable expression of shRNAmir

Due to the considerably long half-life of the CcO complex [2] and the relatively large amount of material required for subsequent analyses, a stable vector-based RNAi approach was utilized to downregulate the expression of Cox4, Cox5a and Cox6a in HEK293 cells. We designed and constructed 13, 9 and 11 pCMV-GIN-ZEO derivatives encoding miR-30–based shRNAs (shRNAmirs) targeting human *COX4I1*, *COX5A* and *COX6A1* mRNAs, respectively. These plasmids were used to generate stable knockdown (KD) in HEK293 cells. Six out of the 33 produced cell lines, which were found with substantially lower levels of the target proteins, were selected for further analyses (Fig. 1B).

The residual levels of the target subunits in mitochondrial preparations were quantified using denaturing western blots. Serial dilutions of protein isolated from the mitochondria of control line expressing non-silencing shRNA were loaded on the same gels as the knockdown samples so that the steady-state levels of the respective polypeptides in KD cells could be assessed as a percentage of the control values (Fig. S1). The residual amount of the Cox4 polypeptide was found to be 45% in COX4I1 (sh1) and 55% in COX4I1 (sh14) mitochondria. In the COX5A (sh5) and COX5A (sh7) samples, the amount of Cox5a polypeptide was decreased to 35% and 20%, respectively. The Cox6a1 polypeptide was decreased to 25% and 35% in COX6A1 (sh11) and COX6A1 (sh12) mitochondria, respectively.

Relative normalized mRNA levels ($2^{-\Delta\Delta Ct}$ *100) of the major *COX4I1* and minor *COX4I2* isoform were 33% and 24% in the COX4I1 (sh1) sample, and 18% and 77% in the COX4I1 (sh14) sample, respectively. The relative normalized levels of the major *COX6A1* and minor *COX6A2* isoform mRNA accounted for 13% and 21% in the COX6A1 (sh11) sample, and 12% and 105% in the COX6A1 (sh12) sample, respectively.

Steady-state levels of a subset of respiratory chain subunits as well as several other mitochondrial proteins are not affected in COX4, COX5A and COX6A KD cells

The mitochondrial preparations used to quantify target subunits were utilized for SDS-PAGE immunodetection to determine the steady-state levels of selected CcO subunits, representative respiratory chain subunits and several other mitochondrial proteins (Fig. S1).

Depletion of subunit Cox4 led to a reduction in the level of Cox5a to 45% in COX4I1 (sh1) and 55% in COX4I1 (sh14) samples as compared to control. The levels of Cox1 and Cox2 were both 80 and 90% of the control values in COX4I1 samples (sh1) and (sh14), respectively. Depletion of subunit Cox5a resulted in a decrease in the levels of Cox4 and Cox2 to 35% in COX5A (sh5) and 20% in COX5A (sh7), whereas the level of Cox1 remained unchanged. Downregulation of subunit Cox6a caused a reduction in the levels of subunits Cox1, Cox2, Cox4 and Cox5a to 80% of the control values. The steady-state levels of the pyruvate dehydrogenase subunit E2 (PDH-E2), porin, cytochrome *c*, the 70-kDa flavoprotein subunit of the succinate:ubiquinone reductase complex (SDHA), the ATP synthase subunit F1-β (ATPase F1-β), complex III core protein 2 and the complex I subunit NDUFA9 were not changed as compared to control.

Depletion of subunits Cox4, Cox5a and Cox6a1 decreases the quantity of CcO holoenzyme and increases an accumulation of CcO subcomplexes

To study the impact of the depletion of subunits Cox4, Cox5a and Cox6a on CcO holoenzyme levels, we performed 5-15% BN-PAGE western blot analyses. The same mitochondrial fractions used for SDS-PAGE western blots were solubilized in DDM and analyzed along with serial dilutions of control samples (Fig. 2A). The amount of CcO holoenzyme was diminished to 65% of the control value in COX4I1 (sh1) and to 75% of the control value in COX4I1 (sh14) samples. The COX5A KD samples (sh7) and (sh5) showed a decrease in the amount of the CcO holoenzyme to 20% and 60% of the control values,

respectively. In COX6A1 (sh11) and COX6A1 (sh12) samples, CcO holoenzyme was reduced to 25% and 30% of the control values, respectively.

To investigate the assembly pattern of CcO, we performed BN-PAGE as well as two-dimensional BN/SDS-PAGE, in which we utilized 8-16% polyacrylamide gradients followed by western blot analysis of the selected subunits. The BN anti-Cox1 immunoblots revealed the presence of several distinct bands in knockdown mitochondria, which were termed *a-e* (Fig. 2B). The holoenzyme band *a* was, in fact, found to be composed of two bands (a_1 and a_2) [18]. COX6A1 KD mitochondria showed a reduction in the levels of both bands a_1 and a_2 to 20% of the control values (Fig. 2B, C). In contrast, the decrease in band a_1 in COX4 and COX5A KD samples, which was comparable to that for COX6A1 mitochondria, was accompanied by a more profound reduction in the amount of band a_2 (Fig. 2B, C). In addition to band *a*, anti-Cox1 immunoblotting detected three faster migrating bands (*b*, *x* and *c*) in all samples with approximate molecular weights of 180, 155 and 110 kDa, respectively. Band *b*, which was barely discernible between control, COX4 KD and COX5A KD mitochondria, was increased in COX6A samples (Fig. 2B). This band very likely represents the previously identified assembly intermediate S3 (Fig. 2D) [2]. Band *x*, which was almost undetectable in controls and slightly increased in COX6A mitochondria, was markedly increased in the COX5A (sh7) sample. Despite its high apparent molecular weight, this band was detectable only with the anti-Cox1 antibody. Band *c*, which was detected in all samples, was increased in COX4 and COX5A KD mitochondria. This band was detected with antibodies to Cox1, Cox4 and Cox5a in COX6A1 KD samples, but only with the anti-Cox1 antibody in COX4 and COX5A KD samples (Fig. 2D). Finally, bands *d* and *e*, with approximate molecular weights of 100 and 85 kDa, respectively, were found only in COX4 and COX5A samples. These bands were increased in the severely CcO-deficient COX5A sample (sh7) and were detected exclusively with the anti-Cox1 antibody.

Whereas CcO activity is significantly decreased, activities of respiratory chain complexes I, II and III are not affected in COX5A and COX6A1 KD cells

To assess residual CcO activity in mitochondrial preparations, we determined CcO activity and normalized it to the activity of complex II (SQR) (Fig. 1B). The same mitochondrial preparations used in the electrophoretic analyses were utilized in these assays. The relative CcO/SQR ratio values obtained for mitochondria from the COX4I1 (sh1) (97%) and COX4I1 (sh14) (103%) cells were comparable to that obtained for control cells. In COX5A (sh5) and COX5A (sh7) mitochondria, the relative normalized CcO/SQR ratio accounted for 72% and 57% of the control values, respectively. The mitochondrial preparations from COX6A1 (sh11) and COX6A1 (sh12) cells revealed a decrease in the CcO/SQR ratio to 51% and 73% of the control values, respectively. The activities of the remaining respiratory chain complexes were found to be unchanged in all of the knockdown samples investigated (data not shown).

Isolated CcO deficiency due to knockdown of COX5A and COX6A1 affects the organization of respiratory supercomplexes in HEK293 cells

To study the impact of COX5A and COX6A1 KD on the composition of respiratory chain supercomplexes, mitochondrial fractions were solubilized with digitonin (digitonin/protein ratio 6 g/g) and analyzed by BN/SDS-PAGE and BN/BN-PAGE western blotting. Both approaches showed that COX5A and COX6A1 knockdown significantly decreased the levels of the dimeric form of the CcO holoenzyme (Fig. 3A, B). Furthermore, BN/BN-PAGE western blots revealed markedly reduced levels of supercomplexes III_2IV_2 and $I_1III_2IV_2$, which apparently contained the dimeric form of the CcO holoenzyme (Fig. 3B). In contrast, the amount of the major mammalian supercomplex $I_1III_2IV_1$ was normal or slightly

increased (Fig. 3B). The appearance of the faint spot corresponding to undissociated IV_2 below the spot corresponding to III_2 of the III-IV-containing supercomplex substantiates the presence of the III_2IV_2, rather than the III_2IV_1 supercomplex in the samples (Fig. 3B, long exposure). The two spots migrating above complex I likely represent undissociated supercomplexes (e.g., $I_1III_2IV_1$ and I_1IV_1) [19].

In all samples, including the controls, BN/BN-PAGE immunoblots revealed additional spots that migrated at the level of supercomplexes in the first dimension, but had apparent molecular weights lower than that of the CcO holoenzyme (Fig. 3B). These spots were most apparent in COX5A KD mitochondria, which exhibited the most severe CcO holoenzyme defect and the highest accumulation of incomplete CcO assemblies (Fig. 2B). Indeed, these spots might represent CcO assembly intermediates already in the form of respiratory supercomplexes.

Normal normoxic respiration is accompanied by increased P_{50} values in COX5A and COX6A1 KD cells

To further characterize mitochondrial respiratory function in COX5A (sh7) and COX6A1 (sh11) KD cells, we performed high-resolution respirometry using the OROBOROS oxygraph. The only difference observed in this assay was diminished oxygen consumption (~80% of control) after the addition of ascorbate/TMPD substrates in COX5A (sh7) cells (Fig. 4A). Therefore, we analyzed the respiratory response of the cells to low oxygen. The digitonin-permeabilized cells were treated with FCCP to uncouple and maximally stimulate respiration (state 3u) and then treated with succinate. The oxygen kinetics were quantified by the partial pressure of oxygen at the half-maximal respiration rate (P_{50}). The average P_{50} value was 0.072 ± 0.02 (SD) kPa (n=6) in control (non-silencing) cells, 0.163 ± 0.01 (SD) kPa (n=5) in COX5A (sh7) cells and 0.105 ± 0.01 (SD) kPa (n=3) in COX6A1 (sh11) sample (Fig. 4B). Thus, the P_{50} value was elevated by more than two-fold in COX5A (sh7) and ~1.5-fold in COX6A1 (sh11) cells.

Overexpression of the Cox6a2 isoform complements the quantitative CcO holoenzyme defect of COX6A1 KD cells

Despite the substantial decrease in CcO holoenzyme levels, the levels of heart/muscle-specific *COX6A2* mRNA remained low in Cox6a1-depleted, CcO-deficient cells (Fig. 1A). Therefore, we tested whether the Cox6a2 isoform can substitute for subunit Cox6a1 during CcO assembly in HEK293 cells. To obtain optimal accumulation of the subunit polypeptide, the cells were transfected twice consecutively, leading to transgene expression for a total of four days. Both untagged and FLAG-tagged forms were used to transfect wild-type and COX6A1 KD cells. This analysis was simplified by the fact that both COX6A1 shRNAmirs used to prepare the KD cells targeted the 3´UTR of COX6A1 mRNA, which was not present in our Cox6a2 expression constructs.

The ectopic expression of the Cox6a2 isoform in COX6A1 (sh11) cells led to the restoration of wild-type CcO levels. The total pool of CcO in these cells consisted of the Cox6a2-containing enzyme as well as residual Cox6a1-containing molecules (~25%) (Fig. 5B). Therefore, both untagged (Fig. 5A, B) and FLAG-tagged (Fig. 5A, C) Cox6a2 polypeptides could substitute for the Cox6a1 isoform during CcO assembly in HEK293 cells. From these experiments, it was also apparent that ectopic expression of Cox6a2 in wild-type HEK293 cells increased the amount of CcO holoenzyme (band a_1) as well as the level of band a_2. In all transfected samples, including controls, an increase in the amount of the assembly intermediate S3 (band *b*) was observed, probably as a result of the transfection treatment (Fig. 5A, B).

The consequences of increased CcO content after ectopic expression of the Cox6a2 isoform in COX6A1 KD cells were analyzed by spectrophotometric measurement of CcO activity. CcO activity in COX6A2-FLAG expressing cells, which was normalized to the activity of the control enzyme (SQR, complex II), did not changed significantly as compared to either untreated wild-type cells or wild-type cells transfected with the control vector (1.26-1.29). In COX6A1 KD cells, ectopic expression of the COX6A2 - FLAG isoform led to a ~1.5-fold increase in CcO/SQR activity ratio as compared to transfection with the control vector (CcO/SQR ratio was 0.75 and 0.49, respectively) (Fig. 5D).

Subunit Cox7a2 enters the CcO assembly after Cox7b, but before Cox6a2

To elucidate the entry points of subunits Cox7a2 and Cox7b with respect to the formation of the assembly intermediate S3, which shows increased accumulation in COX6A1 KD cells, we transfected COX6A1 KD cells with expression constructs containing Cox7a2 and Cox7b coding sequences fused to a C-terminal FLAG epitope. To obtain optimal accumulation of the subunit polypeptides, the cells were transfected twice consecutively, leading to transgene expression for a total of four days. Subsequently, isolated mitochondria were resolved by 7-10% BN-PAGE and subjected to western blot analysis using antibodies specific to Cox1 and the FLAG epitope. No changes in the amount of the CcO holoenzyme or S3 intermediate were observed in COX6A1 KD mitochondria upon expression of these polypeptides (Fig. 5C).

In contrast to the anti-Cox1 immunoblot, which detected the S3 intermediate in all of the analyzed samples (Fig. 5C, long exposure of band *b*), the FLAG-specific antibody cross-reacted with this assembly intermediate only in mitochondria from cells expressing Cox7b-FLAG. The fact that Cox1-specific, but not FLAG-specific, antibodies detected S3 in the samples expressing Cox7a2-FLAG indicated that, unlike Cox7b, Cox7a2 is incorporated after the formation of the assembly intermediate S3 (Fig. 5C).

Mitochondrial preparations from cells transfected with the Cox6a2-FLAG construct were also analyzed for the presence of expressed subunits in the late assembly forms of CcO. Despite the high cross-reactivity of both bands a_1 and a_2 with the anti-Cox1 antibody in these samples, the FLAG-specific antibody detected band a_2 only in Cox7a2-FLAG and Cox7b-FLAG expressing samples (Fig. 5C). Furthermore, when endogenous Cox6a1 was probed, only a_1 was detected in samples where both bands a_1 and a_2 were confirmed with antibodies specific to Cox1, Cox2 or Cox6c (Fig. 5A, B). These results indicated that subunit Cox6a is incorporated after the formation of band a_2, probably as the last structural subunit incorporated into the human CcO complex.

DISCUSSION

CcO is a crucial cellular enzyme with a central role in oxidative metabolism [2, 20]. The significant interest in the biogenesis of CcO stems from its clinical importance. Defective CcO biogenesis is frequently related to severe mitochondrial diseases that often involve tissues with high energy demand [2, 21, 22].

It was previously demonstrated in various non-human eukaryotic models that knockdown of Cox4 or Cox5a impacts CcO holoenzyme content [23-26]. Deficiency of subunit Cox6a was described to cause severe CcO deficiency in Drosophila [27] and mice [28]. However, the yeast Cox6a homologue is dispensable for assembly of the yeast CcO complex [29]. Here, we demonstrated that the impact of stable downregulation of COX4I1, COX5A and COX6A1 in human cultured cells on the content of CcO corresponds to similar studies in higher eukaryotes. Our data further provide detailed knockdown-specific patterns of CcO assembly intermediates, and indicate several novel aspects of the sequential incorporation of subunits during the assembly process including identification of a novel assembly intermediate in human CcO assembly.

Overall, the accumulation of CcO subcomplexes seen in our KD cells reflected the proposed entry of individual subunits into the assembly. The effects of COX6A knockdown on CcO subcomplex pattern was manifested mainly by the marked increase in the assembly intermediate S3. Unlike COX4 and COX5A KD mitochondria, in which the reduction in the holoenzyme band a_1 was accompanied by a more pronounced decrease in band a_2, Cox6a-deficient mitochondria retained significantly higher levels of the latter species. These results newly indicate that band a_2 represents another rate-limiting step in human CcO assembly. Both Cox6a and Cox6b subunits, which are thought to be responsible for dimerization of CcO, are the first to dissociate from the bovine complex under various destabilizing conditions [30, 31]. Thus, it appears plausible that the elevated levels of the assembly intermediate S3 in COX6A KD cells could stem from compromised binding of Cox6b, which might be contingent upon the concomitant assembly of Cox6a. Knockdown of both early-assembled subunits Cox4 and Cox5a resulted in accumulation of four subcomplexes consisting merely of subunit Cox1. The absence of Cox1.Cox4/Cox5a heterodimers further confirmed the interdependence of the assembly of Cox4 and Cox5a [11, 32]. Together with the lack of accumulation of higher molecular weight intermediates, our findings suggest that the assembly of the Cox4·Cox5a heterodimer with Cox1 is necessary for the subsequent association of Cox2, and thus, for the rest of the assembly to proceed. The Cox1-containing subcomplex *x* of ~155 kDa, which apparently does not contain any of the CcO subunits that we tested, was found to be particularly increased in COX5A KD mitochondria. The composition and migration of this subcomplex suggests that it might represent an off-path complex that is not relevant to the normal route of assembly. However, the other samples, including controls, contained small amounts of this subcomplex as well. A similar situation in terms of discrepancy between subunit composition and the apparent molecular weight was observed in the case of the 110 kDa subcomplex *c* from COX4 and COX5A KD mitochondria. These results strongly suggest that individual CcO subunits as well as CcO subcomplexes associate during the assembly with several non-subunit proteins, as reported for yeast Cox1 [33]. The expression of FLAG-tagged versions of Cox7a2, Cox7b and Cox6a2 in both wild-type and Cox6a1-deficient backgrounds allowed us to elucidate for the first time the very late events in human CcO assembly. We identified the particular entry points of these three subunits and demonstrated the significance of the CcO holoenzyme bands a_1 and a_2. According to our results, band a_1 very likely represents the 13-subunit CcO holoenzyme (S4). In contrast, band a_2 lacks subunit Cox6a, which appears to be added as the last assembled structural subunit. Band a_2 (S4*) is formed by the addition of Cox7a2 and probably Cox6b1

[18] to the assembly intermediate S3. Finally, subunit Cox7b was found to join the assembling complex during or at the end of the formation of the assembly intermediate S3 (Scheme 1).

The amount of CcO holoenzyme in COX5A (sh7) and both COX6A1 KD samples corresponded to the residual content of the targeted subunits. Based on our assertion that the Cox6a subunit completes the assembly of the CcO holoenzyme, the amount of fully assembled CcO seems to be strictly contingent upon the amount of the residual Cox6a. Furthermore, transient overexpression of Cox6a subunit in wild-type HEK293 cells increased the content of CcO holoenzyme. Lower level of S3 intermediate and a shift in the a_1:a_2 ratio toward a_1 in COX5A (sh7) sample suggest changes in the kinetics of CcO assembly in terms of the increased utilization of intermediates subsequent to the integration of Cox5a, thereby increasing the level of complete CcO complex to the level of Cox5a. A similar reduction in the levels of RNAi-target subunits in COX5A (sh5) and COX6A1 (sh12) cells resulted in a milder reduction of CcO holoenzyme levels in Cox5a-deficient cells. This observation suggests the existence of different threshold values for the availability of various CcO subunits during enzyme assembly. The diminished content of CcO holoenzyme in our KD cells resulted in a milder reduction in specific CcO activity. Indeed, the relatively mild Cox4 reduction in COX4I1 KD cells resulted in virtually normal CcO activity. These observations are in line with the well-established high excess capacity of CcO [20, 34].

Diaz and colleagues demonstrated that the total loss of CcO leads to complex I deficiency in a mouse COX10 knockout model [35]. Furthermore, RNAi knockdown of COX4 in murine cultured cells resulted in decreased stability and activity of complex I [24]. A similar effect of COX4 and COX5A KD on complex I was described in *Caenorhabditis elegans*, where the content of complex I was normal, but its enzymatic activity was significantly reduced [23]. In contrast, the CcO deficiency in our COX4, COX5A and COX6A KD cells did not lead to any significant changes in the amount and/or activity of other complexes of oxidative phosphorylation system, including complex I. Similarly, normal levels and activity of complex I were also found in murine COX5B KD cells with severe CcO deficiency [36]. Further work is needed to establish the potential role of fully assembled CcO in complex I biogenesis.

High-resolution respirometry in our CcO deficient cellular model showed significantly increased P_{50} values. This may indicate either a change in mitochondrial capacity or decreased affinity for oxygen ($=1/P_{50}$) of the residual CcO [20]. The lack of a significant decrease in maximal (state 3u) normoxic respiration in our KD cells argues against the possibility that P_{50} is increased due to lower mitochondrial capacity. The second possibility, which involves a decrease in oxygen affinity in active states when the demand for oxygen is highest, is paradoxical from a functional point of view [20]. However, if the increase in P_{50} is accompanied by a greater increase in maximum flux (J_{max}), the J_{max}/P_{50} ratio still increases and indicates elevated apparent catalytic efficiency with activation by ADP [20]. When plotted as a function of the specific oxygen flux normalized to protein content, the P_{50} values in both our KD cell lines increased without a corresponding increase in oxygen flux (Fig. 4C). Therefore, the increase in P_{50} in our KD cells is most likely due to decreased affinity of CcO for oxygen (increased K´m). Marked CcO deficiency with almost unchanged normoxic cellular respiratory rates accompanied by increased P_{50} values were also found in fibroblasts from patients with Leigh syndrome due to Surf1 deficiency [17]. In addition to reduced holoenzyme levels, Surf1-deficient fibroblasts were characterized by increased accumulation of CcO subcomplexes. It was hypothesized that under conditions of high oxygen pressure, the accumulated subcomplexes could restore near normal respiration, and contribute to the increased P_{50} value [17, 37]. However, it was repeatedly demonstrated that subcomplexes found in SURF1 fibroblasts are devoid of the catalytic core subunit Cox2 [11, 38]. Similar

subcomplexes i.e., devoid of Cox2 also accumulate in COX5A KD mitochondria. Cox2 is known to mediate electrostatic binding of cytochrome *c* and represents the initial entry site for electrons. The subcomplexes in COX6A1 KD cells are represented mainly by incomplete CcO assemblies that lack only few peripheral nuclear-encoded subunits. Exposure of isolated monomeric bovine CcO to hydrostatic pressure results in a mixture of 13-, 11- and 9-subunit CcO complexes [31]. Analysis of separated forms showed that both the 13-subunit complex as well as the 11-subunit form devoid of subunits Cox6a and Cox6b retained 85-90% of electron transport activity of the untreated enzyme. The 9-subunit form that lacks two additional subunits (Cox3 and Cox7a) had only 40-45% activity of intact enzyme. The authors were not able to determine the loss of which of the two subunits led to such marked reduction in enzyme activity [31]. Nevertheless, the results of other studies suggest that the loss of Cox3 is likely responsible for the majority of CcO inactivation observed [39, 40]. Both of the major intermediates found in our Cox6a deficient cells (a_2 and S3) are thus likely to be capable of electron transfer, unlike the subcomplexes from COX5A KD cells. Indeed, the capacity of CcO in COX5A KD cells as measured by oxygen consumption after ascorbate/TMPD was significantly decreased, and the P_{50} value was significantly increased when compared to both control and COX6A1 KD samples. Therefore, it appears likely that the presence of the high molecular weight CcO subcomplexes in COX6A KD cells might contribute to cellular respiration at low oxygen levels and lead to higher apparent CcO excess capacity. In contrast, uncoupled respiration did not change at normoxic levels of oxygen after natural substrates, and spectrophotometric measurement indicated decrease of specific CcO activity to the same extent in both cell lines.

Nonetheless, the decreased oxygen affinity of CcO in both KD cell lines appears paradoxical, as there apparently seems to be no rational reason for the decreased catalytic competence of the residual CcO enzyme. Furthermore, the substantial reduction in CcO content was accompanied by less diminished specific activity of CcO in COX5A and COX6A1 KD cells suggesting compensatory catalytic stimulation of the residual CcO. Taken together, we assume that decreased oxygen affinity of CcO in our KD cells results from quantitative changes in the CcO pool which, when reduced, undergoes normal flux at high oxygen pressure but is significantly more sensitive to decreased oxygen levels. Such an assumption is in line with the previously demonstrated oxygen dependence of CcO flux control [41]. In this study, a lower experimental concentration of oxygen was related to a steeper initial slope of the cyanide titration curve for maximal succinate oxidation rate. Moreover, a lower concentration of CcO inhibitor was necessary to cause complete inhibition of respiration [41].

Both COX5A and COX6A KD mitochondria showed, in addition to a reduction in the CcO monomer, an even more pronounced reduction of the dimeric form of CcO. Indeed, the pattern of respiratory supercomplexes showed that species containing the dimeric form of the CcO complex (III_2IV_2 and $I_1III_2IV_2$) are significantly reduced in KD cells. On the contrary, supercomplexes containing monomeric CcO were unaltered or even slightly increased. A similar effect was recently shown to stem from a CcO defect induced by knockdown of the human CcO-specific copper metallochaperone Cox17 [42]. The majority of mammalian CcO is thought to exist in a dimeric form within the inner mitochondrial membrane [43]. Indeed, it appears that dimerization of CcO plays a crucial structural and functional role, conferring maximal structural stability to the complex [31].

In yeast, it was shown that complex IV associates with complex III already in the form of incomplete subcomplexes, and that some of the late assembled subunits are likely added directly to the III/IV supercomplex [44]. An example of such a subunit is Cox13, the yeast homologue of human Cox6a [45]. Indeed, BN/BN-PAGE immunoblots for both control and downregulated cells revealed additional spots that migrate at the level of supercomplexes in

the first dimension, but with an apparent molecular weight lower than that of the CcO holoenzyme. Although we cannot, in principle, exclude the removal of some of the peripheral subunits due to detergent treatment, these spots might represent incomplete CcO assemblies that are already present in supercomplexes. Further analyses are required to confirm this hypothesis.

Despite remarkable conservation of secondary structure in Cox6a isoforms, mature Cox6a1 and Cox6a2 subunits (non-muscle and heart/muscle isoform) were found to share lower intra-species (approx. 60%) than inter-species (80-88%) amino acid sequence identity in humans, rats and cows, suggesting that the COX6A1 and COX6A2 genes arose prior to mammalian radiation [46]. The tissue-specific pattern of these isoforms is established during tissue differentiation [47-49]. A switch from Cox6a1 to Cox6a2 isoforms was described to occur during mammalian postnatal development in skeletal muscle and heart as well as during differentiation of myogenic cells *in vitro*, and is assumed to be essential for normal function of tissues with high aerobic metabolic demands [48, 49]. In the heart of mice lacking the COX6A2 gene, the content of the CcO holoenzyme was virtually equal to the level of Cox6a1 isoform in wild type control, which accounted for 20% of the total Cox6a content. Thus, the content of CcO comprising Cox6a1 appeared to be unchanged, in other words, without apparent compensation by induction of the expression of subunit Cox6a1 in the knockout heart [28]. HEK293 cells used in this study are derived from embryonic kidney tissue, which is specific by almost exclusive (both prenatal and postnatal) expression of Cox6a1 isoform [47-49]. Indeed, the vast majority of the *COX6A* transcripts in HEK293 cells is represented by the Cox6a1 isoform. The COX6A1 RNAi constructs were designed to target the 3´untranslated region of the COX6A1 transcript, which is missing in the COX6A2 isoform. Indeed, similar to the results from COX6A2-knockout heart, the decrease in the major isoform in our COX6A1 KD cells was not accompanied by upregulation of the minor isoform (COX6A2). However, ectopic expression of Cox6a2 in COX6A1 KD cells tends to complement the CcO defect. Therefore, it appears that the mechanisms responsible for maintenance of tissue-specific patterns of Cox6a isoforms cannot react in response to actual cellular state. In contrast, it is also possible that the pronounced biochemical defect still did not provoke sufficient physiological impairment, which would otherwise trigger the expression of the minor subunit.

In conclusion, our results indicate that whereas nuclear-encoded CcO subunits Cox4 and Cox5a are required for the assembly of the functional CcO complex, the Cox6a subunit is required for the overall stability of the holoenzyme. Consequently, the heterogeneous CcO population of Cox6a deficient cells exhibits higher residual respiration at low oxygen levels than the various CcO forms found in COX5A KD cells. The fact that the ectopic expression of heart/muscle-specific isoform of Cox6a can complement the CcO defect in COX6A1 KD cells is in sharp contrast to unaltered levels of this isoform in our CcO deficient model, and suggests the existence of a fixed differentiation program regarding human Cox6a isoforms. The description of a novel assembly intermediate at the very last step of CcO assembly suggests additional regulatory level of the process. The normal amount and function of complex I in all of our CcO deficient cell lines suggest that even relatively small residual amounts of CcO can maintain normal biogenesis of this respiratory complex in human cells.

FUNDING

This work was supported by grants from the Grant Agency of Charles University [GAUK 1/2006/R], the Grant Agency of Czech Republic [GACR 303/07/0781], the Internal Grant Agency of the Ministry of Health of the Czech Republic [IGA 10581/3] and the Center of Applied Genomics [CAG 1M0520], and by institutional project [MSM 0021620806].

REFERENCES

1 Zhen, Y., Hoganson, C. W., Babcock, G. T. and Ferguson-Miller, S. (1999) Definition of the interaction domain for cytochrome c on cytochrome c oxidase. I. Biochemical, spectral, and kinetic characterization of surface mutants in subunit ii of Rhodobacter sphaeroides cytochrome aa(3). J. Biol. Chem. **274**, 38032-38041

2 Stiburek, L., Hansikova, H., Tesarova, M., Cerna, L. and Zeman, J. (2006) Biogenesis of eukaryotic cytochrome c oxidase. Physiol. Res. **55 Suppl 2**, S27-41

3 Huttemann, M., Lee, I., Pecinova, A., Pecina, P., Przyklenk, K. and Doan, J. W. (2008) Regulation of oxidative phosphorylation, the mitochondrial membrane potential, and their role in human disease. J. Bioenerg. Biomembr. **40**, 445-456

4 Fontanesi, F., Soto, I. C. and Barrientos, A. (2008) Cytochrome c oxidase biogenesis: new levels of regulation. IUBMB Life **60**, 557-568

5 Helling, S., Vogt, S., Rhiel, A., Ramzan, R., Wen, L., Marcus, K. and Kadenbach, B. (2008) Phosphorylation and kinetics of mammalian cytochrome c oxidase. Mol. Cell. Proteomics **7**, 1714-1724

6 Huttemann, M., Kadenbach, B. and Grossman, L. I. (2001) Mammalian subunit IV isoforms of cytochrome c oxidase. Gene **267**, 111-123

7 Kadenbach, B., Huttemann, M., Arnold, S., Lee, I. and Bender, E. (2000) Mitochondrial energy metabolism is regulated via nuclear-coded subunits of cytochrome c oxidase. Free. Radic. Biol. Med. **29**, 211-221

8 Tsukihara, T., Aoyama, H., Yamashita, E., Tomizaki, T., Yamaguchi, H., Shinzawa-Itoh, K., Nakashima, R., Yaono, R. and Yoshikawa, S. (1996) The whole structure of the 13-subunit oxidized cytochrome c oxidase at 2.8 A. Science **272**, 1136-1144

9 Arnold, S. and Kadenbach, B. (1997) Cell respiration is controlled by ATP, an allosteric inhibitor of cytochrome-c oxidase. Eur. J. Biochem. **249**, 350-354

10 Horvat, S., Beyer, C. and Arnold, S. (2006) Effect of hypoxia on the transcription pattern of subunit isoforms and the kinetics of cytochrome c oxidase in cortical astrocytes and cerebellar neurons. J. Neurochem. **99**, 937-951

11 Stiburek, L., Vesela, K., Hansikova, H., Pecina, P., Tesarova, M., Cerna, L., Houstek, J. and Zeman, J. (2005) Tissue-specific cytochrome c oxidase assembly defects due to mutations in SCO2 and SURF1. Biochem. J. **392**, 625-632

12 Schlerf, A., Droste, M., Winter, M. and Kadenbach, B. (1988) Characterization of two different genes (cDNA) for cytochrome c oxidase subunit VIa from heart and liver of the rat. Embo J. **7**, 2387-2391

13 Nijtmans, L. G., Taanman, J. W., Muijsers, A. O., Speijer, D. and Van den Bogert, C. (1998) Assembly of cytochrome-c oxidase in cultured human cells. Eur. J. Biochem. **254**, 389-394

14 Stiburek, L., Fornuskova, D., Wenchich, L., Pejznochova, M., Hansikova, H. and Zeman, J. (2007) Knockdown of human Oxa1l impairs the biogenesis of F1Fo-ATP synthase and NADH:ubiquinone oxidoreductase. J. Mol. Biol. **374**, 506-516

15 Wittig, I., Braun, H. P. and Schagger, H. (2006) Blue native PAGE. Nat. Protoc. **1**, 418-428
16 Lowry, O. H., Rosebrough, N. J., Farr, A. L. and Randall, R. J. (1951) Protein measurement with the Folin phenol reagent. J. Biol. Chem. **193**, 265-275
17 Pecina, P., Gnaiger, E., Zeman, J., Pronicka, E. and Houstek, J. (2004) Decreased affinity for oxygen of cytochrome-c oxidase in Leigh syndrome caused by SURF1 mutations. Am. J. Physiol. Cell. Physiol. **287**, C1384-1388
18 Massa, V., Fernandez-Vizarra, E., Alshahwan, S., Bakhsh, E., Goffrini, P., Ferrero, I., Mereghetti, P., D'Adamo, P., Gasparini, P. and Zeviani, M. (2008) Severe infantile encephalomyopathy caused by a mutation in COX6B1, a nucleus-encoded subunit of cytochrome c oxidase. Am. J. Hum. Genet. **82**, 1281-1289
19 Schagger, H. and Pfeiffer, K. (2000) Supercomplexes in the respiratory chains of yeast and mammalian mitochondria. Embo J. **19**, 1777-1783
20 Gnaiger, E., Lassnig, B., Kuznetsov, A., Rieger, G. and Margreiter, R. (1998) Mitochondrial oxygen affinity, respiratory flux control and excess capacity of cytochrome c oxidase. J. Exp. Biol. **201**, 1129-1139
21 Diaz, F. Cytochrome c oxidase deficiency: patients and animal models. Biochim. Biophys. Acta **1802**, 100-110
22 Shoubridge, E. A. (2001) Cytochrome c oxidase deficiency. Am. J. Med. Genet. **106**, 46-52
23 Suthammarak, W., Yang, Y. Y., Morgan, P. G. and Sedensky, M. M. (2008) Complex I function is defective in complex IV-deficient Caenorhabditis elegans. J. Biol. Chem.
24 Li, Y., D'Aurelio, M., Deng, J. H., Park, J. S., Manfredi, G., Hu, P., Lu, J. and Bai, Y. (2007) An assembled complex IV maintains the stability and activity of complex I in mammalian mitochondria. J. Biol. Chem. **282**, 17557-17562
25 Baden, K. N., Murray, J., Capaldi, R. A. and Guillemin, K. (2007) Early developmental pathology due to cytochrome c oxidase deficiency is revealed by a new zebrafish model. J. Biol. Chem. **282**, 34839-34849
26 Poyton, R. O., Trueblood, C. E., Wright, R. M. and Farrell, L. E. (1988) Expression and function of cytochrome c oxidase subunit isologues. Modulators of cellular energy production? Ann. N Y Acad. Sci. **550**, 289-307
27 Liu, W., Gnanasambandam, R., Benjamin, J., Kaur, G., Getman, P. B., Siegel, A. J., Shortridge, R. D. and Singh, S. (2007) Mutations in cytochrome c oxidase subunit VIa cause neurodegeneration and motor dysfunction in Drosophila. Genetics **176**, 937-946
28 Radford, N. B., Wan, B., Richman, A., Szczepaniak, L. S., Li, J. L., Li, K., Pfeiffer, K., Schagger, H., Garry, D. J. and Moreadith, R. W. (2002) Cardiac dysfunction in mice lacking cytochrome-c oxidase subunit VIaH. Am. J. Physiol. Heart Circ. Physiol. **282**, H726-733
29 Taanman, J. W. and Capaldi, R. A. (1993) Subunit VIa of yeast cytochrome c oxidase is not necessary for assembly of the enzyme complex but modulates the enzyme activity. Isolation and characterization of the nuclear-coded gene. J. Biol. Chem. **268**, 18754-18761
30 Sedlak, E. and Robinson, N. C. (2009) Sequential dissociation of subunits from bovine heart cytochrome C oxidase by urea. Biochemistry **48**, 8143-8150
31 Stanicova, J., Sedlak, E., Musatov, A. and Robinson, N. C. (2007) Differential stability of dimeric and monomeric cytochrome c oxidase exposed to elevated hydrostatic pressure. Biochemistry **46**, 7146-7152
32 Barrientos, A., Gouget, K., Horn, D., Soto, I. C. and Fontanesi, F. (2009) Suppression mechanisms of COX assembly defects in yeast and human: insights into the COX assembly process. Biochim. Biophys. Acta **1793**, 97-107

33 Khalimonchuk, O., Bestwick, M., Meunier, B., Watts, T. C. and Winge, D. R. Formation of the redox cofactor centers during Cox1 maturation in yeast cytochrome oxidase. Mol. Cell. Biol. **30**, 1004-1017

34 Rossignol, R., Faustin, B., Rocher, C., Malgat, M., Mazat, J. P. and Letellier, T. (2003) Mitochondrial threshold effects. Biochem. J. **370**, 751-762

35 Diaz, F., Fukui, H., Garcia, S. and Moraes, C. T. (2006) Cytochrome c oxidase is required for the assembly/stability of respiratory complex I in mouse fibroblasts. Mol. Cell. Biol. **26**, 4872-4881

36 Galati, D., Srinivasan, S., Raza, H., Prabu, S. K., Hardy, M., Chandran, K., Lopez, M., Kalyanaraman, B. and Avadhani, N. G. (2009) Role of nuclear-encoded subunit Vb in the assembly and stability of cytochrome c oxidase complex: implications in mitochondrial dysfunction and ROS production. Biochem. J. **420**, 439-449

37 Pecina, P., Capkova, M., Chowdhury, S. K., Drahota, Z., Dubot, A., Vojtiskova, A., Hansikova, H., Houst'kova, H., Zeman, J., Godinot, C. and Houstek, J. (2003) Functional alteration of cytochrome c oxidase by SURF1 mutations in Leigh syndrome. Biochim. Biophys. Acta **1639**, 53-63

38 Williams, S. L., Valnot, I., Rustin, P. and Taanman, J. W. (2004) Cytochrome c oxidase subassemblies in fibroblast cultures from patients carrying mutations in COX10, SCO1, or SURF1. J. Biol. Chem. **279**, 7462-7469

39 Bratton, M. R., Pressler, M. A. and Hosler, J. P. (1999) Suicide inactivation of cytochrome c oxidase: catalytic turnover in the absence of subunit III alters the active site. Biochemistry **38**, 16236-16245

40 Penttila, T. (1983) Properties and reconstitution of a cytochrome oxidase deficient in subunit III. Eur. J. Biochem. **133**, 355-361

41 Wiedemann, F. R. and Kunz, W. S. (1998) Oxygen dependence of flux control of cytochrome c oxidase -- implications for mitochondrial diseases. FEBS Lett. **422**, 33-35

42 Oswald, C., Krause-Buchholz, U. and Rodel, G. (2009) Knockdown of human COX17 affects assembly and supramolecular organization of cytochrome c oxidase. J. Mol. Biol. **389**, 470-479

43 Musatov, A. and Robinson, N. C. (2002) Cholate-induced dimerization of detergent- or phospholipid-solubilized bovine cytochrome C oxidase. Biochemistry **41**, 4371-4376

44 Mick, D. U., Wagner, K., van der Laan, M., Frazier, A. E., Perschil, I., Pawlas, M., Meyer, H. E., Warscheid, B. and Rehling, P. (2007) Shy1 couples Cox1 translational regulation to cytochrome c oxidase assembly. Embo J. **26**, 4347-4358

45 Brandner, K., Mick, D. U., Frazier, A. E., Taylor, R. D., Meisinger, C. and Rehling, P. (2005) Taz1, an outer mitochondrial membrane protein, affects stability and assembly of inner membrane protein complexes: implications for Barth Syndrome. Mol. Biol. Cell **16**, 5202-5214

46 Fabrizi, G. M., Sadlock, J., Hirano, M., Mita, S., Koga, Y., Rizzuto, R., Zeviani, M. and Schon, E. A. (1992) Differential expression of genes specifying two isoforms of subunit VIa of human cytochrome c oxidase. Gene **119**, 307-312

47 Bonne, G., Seibel, P., Possekel, S., Marsac, C. and Kadenbach, B. (1993) Expression of human cytochrome c oxidase subunits during fetal development. Eur. J. Biochem. **217**, 1099-1107

48 Kim, K., Lecordier, A. and Bowman, L. H. (1995) Both nuclear and mitochondrial cytochrome c oxidase mRNA levels increase dramatically during mouse postnatal development. Biochem. J. **306 (Pt 2)**, 353-358

49 Taanman, J. W., Herzberg, N. H., De Vries, H., Bolhuis, P. A. and Van den Bogert, C. (1992) Steady-state transcript levels of cytochrome c oxidase genes during human myogenesis indicate subunit switching of subunit VIa and co-expression of subunit VIIa isoforms. Biochim. Biophys. Acta **1139**, 155-162

FIGURE LEGENDS

Figure 1. The levels of COX4 and COX6A mRNAs and the effects of shRNA knockdown of COX4I1, COX5A and COX6A1 in HEK293 cells

(**A**) mRNA levels of COX4 and COX6A isoforms in control and COX4 and COX6A1 KD HEK293 cells, normalized to the level of *TBP* mRNA ($2^{-\Delta Ct}$). (**B**) The relationship between the residual target subunit, content of CcO and its enzyme activity. The residual level of the target subunit was determined by SDS-PAGE of mitochondrial protein samples (~30 μg) and western blot. The amount of CcO holoenzyme was determined by 5-15% BN-PAGE (~20 μg) of mitochondrial proteins solubilized by 1.1% dodecyl maltoside (4.8 g/g dodecyl maltoside/protein) followed by western blot. Immunoreactive material was visualized by chemiluminescence. For the loading control, the amount of target subunit was normalized to that of subunit SDHA of complex II and to the outer membrane protein porin. The amount of CcO holoenzyme was normalized to that of complex II. The final values are expressed relatively to control (NS) sample, which was arbitrarily set at 100%. The CcO activity was determined by measuring the rate of cytochrome *c* oxidation (nmol/min/mg of mitochondrial protein) and normalized to the activity of complex II (SQR) (CcO/SQR ratio), which was determined by measuring the rate of 2,6-dichloroindophenol oxidation (nmol/min/mg of mitochondrial protein). For comparison to the level of RNAi-target subunit and CcO content, the CcO/SQR ratio of the mean activity values was, in turn, expressed relative to the CcO/SQR ratio value obtained in the control (NS) sample, which was arbitrarily set at 100%. NS: mitochondria from HEK293 cells expressing the non-silencing control shRNAmir.

Figure 2. The levels of CcO holoenzyme and the assembly pattern of CcO in COX4, COX5A and COX6A1 KD mitochondria

(**A**) Equal amounts (~20 μg) of mitochondrial protein prepared by solubilization at 1.1% dodecyl maltoside (4.8 g/g dodecyl maltoside/protein) and serial dilutions of non-silencing control samples (NS) were resolved by 5-15% BN-PAGE and subjected to western blot analysis with an anti-Cox1 antibody. (**B**) Mitochondrial proteins (~25 μg) prepared by solubilization at 1.1% dodecyl maltoside (4.8 g/g dodecyl maltoside/protein) were resolved by 8-16% BN-PAGE and subjected to western blot analysis with an anti-Cox1 antibody. Both short (up) and long (down) exposures are shown. Equal loading was verified using antibodies to the complex II subunit SDHA and the complex III subunit Core 2 (A, B). (**C**) The same protein samples as (B) were fractionated using 7-10% BN-PAGE and subjected to western blot analysis with an anti-Cox1 antibody. The amount of protein loaded per lane was normalized to the signal of the holoenzyme band a_1. (**D**) The same protein samples as (B) (~35 μg) were resolved by two-dimensional 8-16%/13% BN/SDS-PAGE and subjected to western blot analysis with a cocktail of antibodies specific for subunits Cox1, Cox2, Cox4 and Cox5a. The migration direction of the first, native (BN-PAGE) and the second, denaturing (SDS-PAGE) dimension are marked with gray arrows. The positions of bands *a-e* and the molecular weight (MW) of complex II (123 kDa), the SDHA.SDHB subcomplex (97 kDa) and SDHA (70 kDa) are indicated. Both short and long Cox1-specific exposures are shown. Immunoreactive material was visualized by chemiluminescence (A-D).

Figure 3. Supramolecular organization of CcO in COX5A and COX6A1 KD cells

(**A**) Digitonin-solubilized (6 g/g, digitonin/protein) mitochondrial proteins were separated by 5-12%/10% BN/SDS-PAGE (~45 μg) and subjected to western blot analysis with antibodies specific for the complex III subunit Core 1 and the complex IV subunit Cox1. IV_{Dim} and III_{Dim} indicate complex IV and III homodimers, respectively, and IV_{Sub} indicates CcO subcomplexes. The migration direction of the first, native (BN-PAGE) and the second,

denaturing (SDS-PAGE) dimension are indicated with gray arrows. (**B**) The same protein preparations as in (A) (~45 μg) were fractionated using two dimensional 4-13%/4-15% BN/BN-PAGE and subjected to western blot analysis with a cocktail of antibodies specific for the complex I subunit NDUFB6, the complex III subunit Core 1 and the complex IV subunit Cox1. The migration direction of the first (dig) and the second (DDM) dimension are indicated with gray arrows. Complexes from the first BN-PAGE that retained their masses after 2D BN-PAGE are found on a diagonal. Supercomplexes that dissociated into individual complexes were detected below the diagonal. The small arrows indicate supramolecular assemblies of respiratory complexes that did not dissociate in the second dimension. Asterisks indicate undissociated supercomplexes of higher molecular weights than complex I. Arrowheads denote spots migrating in the first dimension at the level of supercomplexes, but with apparent molecular weights lower than that of the CcO holoenzyme. Immunoreactive material was visualized by chemiluminescence (A-B).

Figure 4. High-resolution respirometry in permeabilized (digitonin-treated), uncoupled (FCCP-treated) COX5A and COX6A1 KD cells.

(**A**) Respiration at environmental normoxic levels of oxygen. The mean rate of oxygen consumption (pmol O_2/s/mg of protein) in KD cells was expressed relative to non-silencing control (NS) mean value, which was arbitrarily set at 100%. GM: relative respiration after addition of glutamate and malate (rotenone-sensitive), GMS: relative respiration after addition of glutamate, malate and succinate (antimycin A-sensitive), S: relative respiration after addition of succinate (antimycin A-sensitive), aT: relative respiration after addition of ascorbate and TMPD (sodium azide-sensitive). (**B**) Mean P_{50} values in cells supplied by succinate. P_{50} represents partial pressure of oxygen at the half-maximal respiration rate. Error bars in (A) and (B) indicate SD. (**C**) The relation of P_{50} and protein-specific oxygen flux. P_{50} values from individual measurements were plotted as a function of protein-specific oxygen flux (J_{max}). ◇: control sample (NS), ▲: COX5A (sh7) KD cells, ■: COX6A1 (sh11) KD cells. $*P < 0.05$, $**P < 0.01$, $***P < 0.001$.

Figure 5. Expression of FLAG-tagged versions of Cox6a2, Cox7a2 and Cox7b in wild-type and COX6A1 KD HEK293 cells

(**A, B**) Equal amounts (~20-50 μg) of mitochondrial protein were solubilized by 1.1% dodecyl maltoside (4.8 g/g dodecyl maltoside/protein) and resolved by 7-10% BN-PAGE and subjected to western blot analysis with antibodies specific to Cox1 (**A**), Cox2, Cox6c and Cox6a1 (**B**). NS: mitochondria from stable HEK293 cells expressing the non-silencing control shRNAmir. Wt: mitochondria form wild-type HEK293 cells. Wt - COX6A2: mitochondria from wild type HEK293 cells transiently transfected with a construct encoding the Cox6a2 subunit. COX6A1 (sh11) - COX6A2: mitochondria from stable COX6A1 (sh11) KD cells transiently transfected with a construct encoding the Cox6a2 subunit. Wt - COX6A2 - FLAG: mitochondria from wild type HEK293 cells transiently transfected with a construct encoding the FLAG epitope-tagged Cox6a2 subunit. COX6A1 (sh11) or (sh12) - COX6A2 - FLAG: mitochondria from stable COX6A1 (sh11) or (sh12) KD cells transiently transfected with a construct encoding the FLAG epitope-tagged Cox6a2 subunit. NS - pmaxFP-Red-N: mitochondria from NS cells transiently transfected with control plasmid pmaxFP-Red-N encoding a fluorescent marker. (**C**) Equal amounts of mitochondrial protein solubilized with 1.1% dodecyl maltoside (5 g/g dodecyl maltoside/protein) were resolved by 7-10% BN-PAGE and subjected to western blot analysis with antibodies specific to the Cox1 subunit (~20 μg of protein loaded per lane) and FLAG epitope (~60 μg of protein loaded per lane). Wt: mitochondria form wild-type HEK293 cells. Wt - COX7A2-FLAG: mitochondria from wild type HEK293 cells transiently transfected with a construct encoding the FLAG epitope-

tagged Cox7a2 subunit. COX6A1 (sh11) - COX7A2 - FLAG: mitochondria from stable COX6A1 (sh11) KD cells transiently transfected with a construct encoding the FLAG epitope-tagged Cox7a2 subunit. Wt - COX7B - FLAG: mitochondria from wild type HEK293 cells transiently transfected with a construct encoding the FLAG epitope-tagged Cox7b subunit. COX6A1 (sh11) - COX7B - FLAG: mitochondria from stable COX6A1 (sh11) KD cells transiently transfected with a construct encoding the FLAG epitope-tagged Cox7b subunit. Both short and long exposures are shown. (**A-C**) Equal loading was verified using an antibody to the complex II subunit SDHA. Positions of the various assembly forms of complex IV (a, b) and holoenzyme of complex II (C II) as well as specificity of the antibodies (in the right hand margin) are indicated. Immunoreactive material was visualized by chemiluminescence. (**D**) CcO activity was determined by measuring the rate of cytochrome *c* oxidation (nmol/min/mg of mitochondrial protein) and normalized to the activity of complex II (SQR) (CcO/SQR ratio), which was determined by measuring the rate of 2,6-dichloroindophenol oxidation (nmol/min/mg of mitochondrial protein). Wt: mitochondria from wild-type HEK293 cells. Wt - pmaxFP-Red-N: mitochondria from wt cells transiently transfected with control plasmid pmaxFP-Red-N encoding a fluorescent marker. Wt - COX6A2 - FLAG: mitochondria from wild type HEK293 cells transiently transfected with a construct encoding the FLAG epitope-tagged Cox6a2 subunit. COX6A1 (sh11) - pmaxFP-Red-N: mitochondria from stable COX6A1 (sh11) KD cells transiently transfected with control plasmid pmaxFP-Red-N encoding a fluorescent marker. COX6A1 (sh11) - COX6A2 - FLAG: mitochondria from stable COX6A1 (sh11) KD cells transiently transfected with a construct encoding the FLAG epitope-tagged Cox6a2 subunit.

SCHEME LEGEND

Scheme 1. Proposed model of the mammalian CcO assembly pathway

Prosthetic groups and assembly factors are indicated. Arabic numerals denote CcO subunits within subcomplexes. S2 and S3 indicate previously identified assembly intermediates. S4 represents the 13-subunit CcO holoenzyme, and S4* indicates the late assembly intermediate that immediately precedes the formation of the holoenzyme (see text for details).

Figure 1

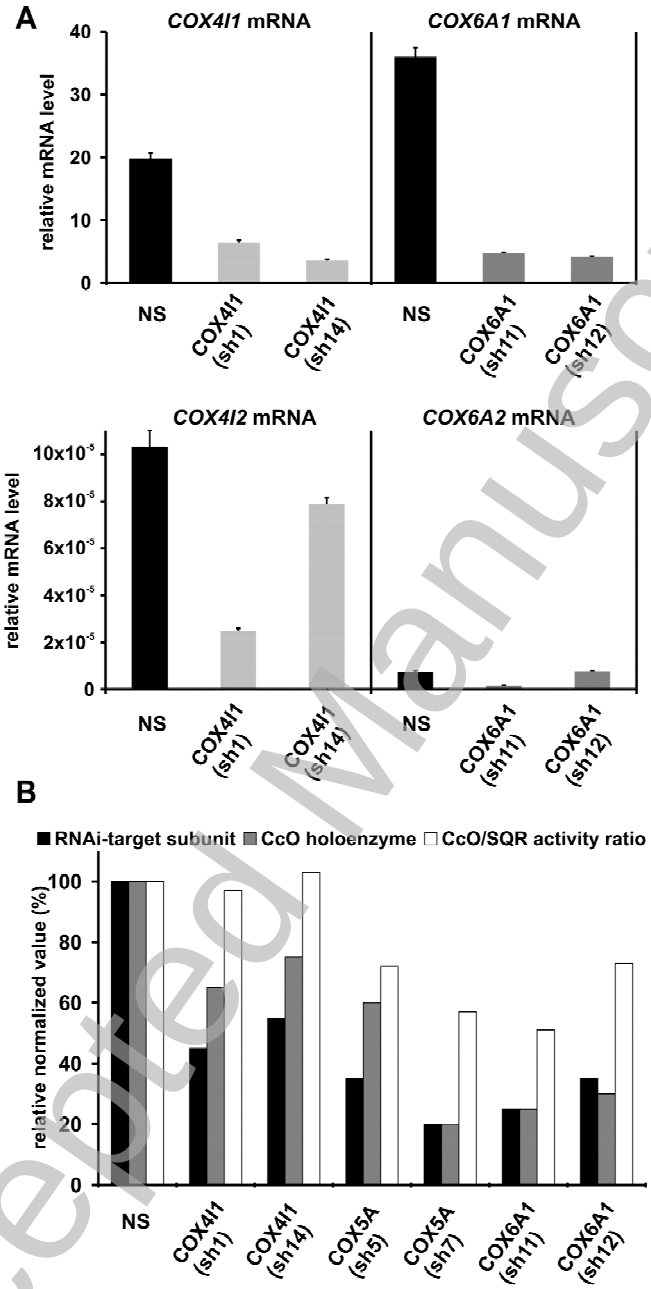

Biochemical Journal Immediate Publication. Published on 22 Mar 2010 as manuscript BJ20091714

Figure 2

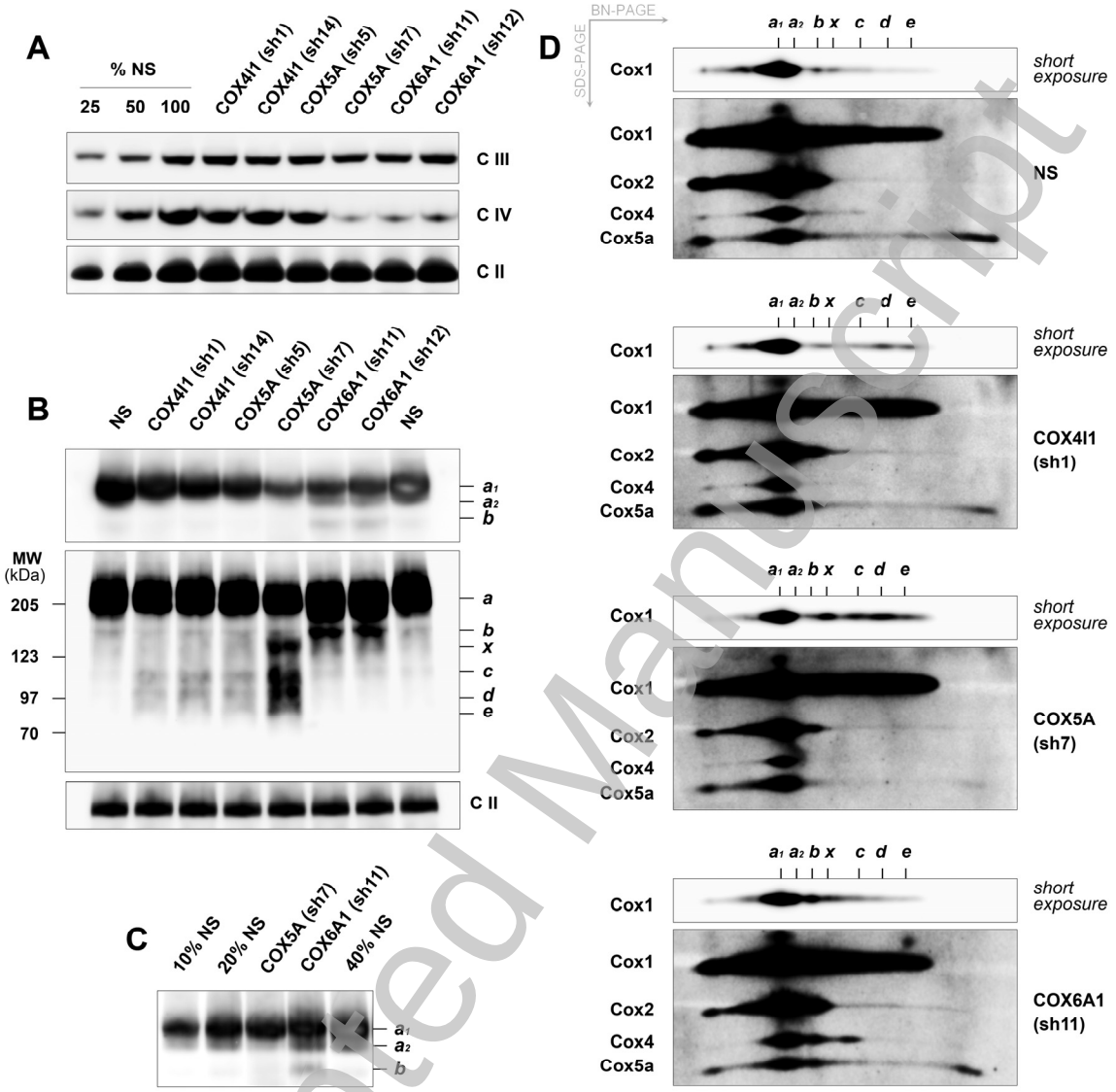

Figure 3

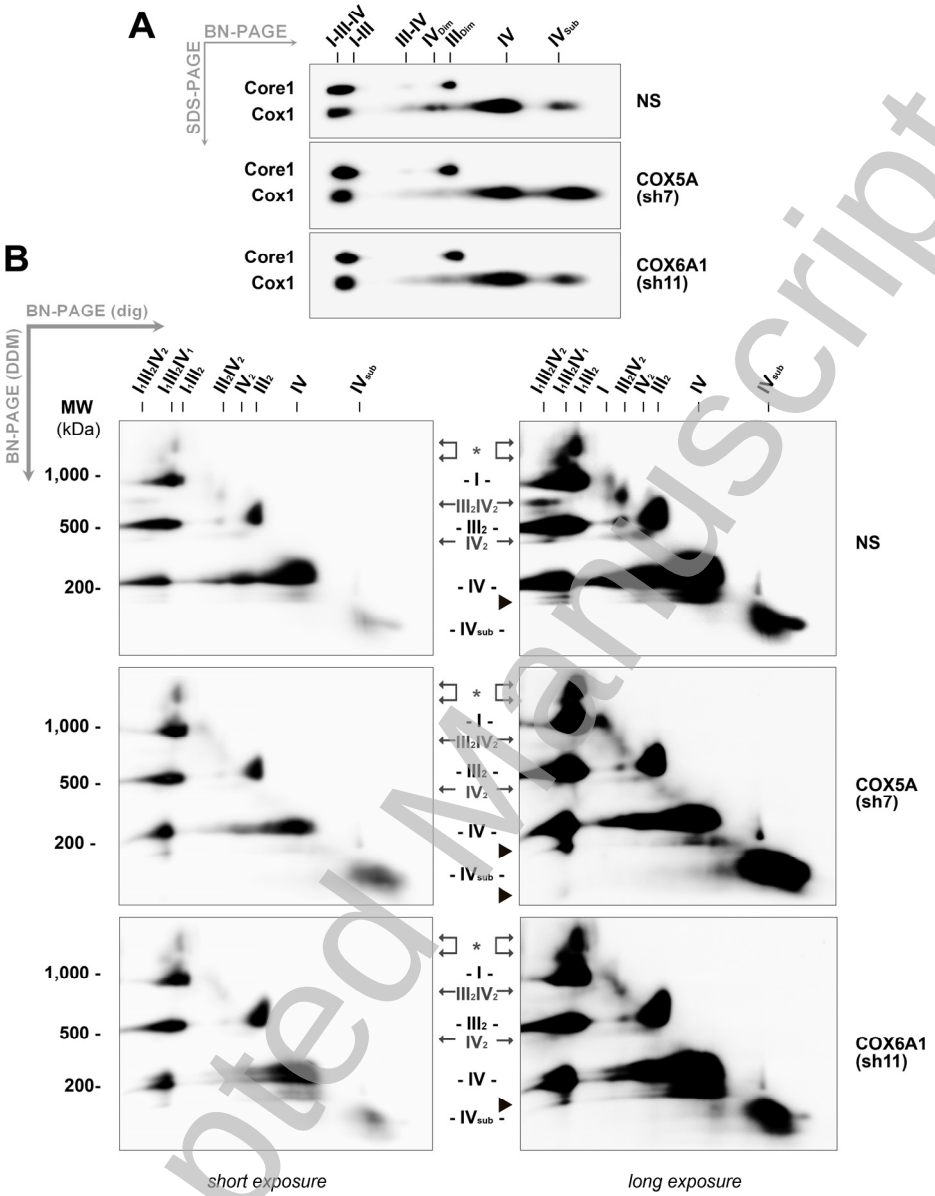

Figure 4

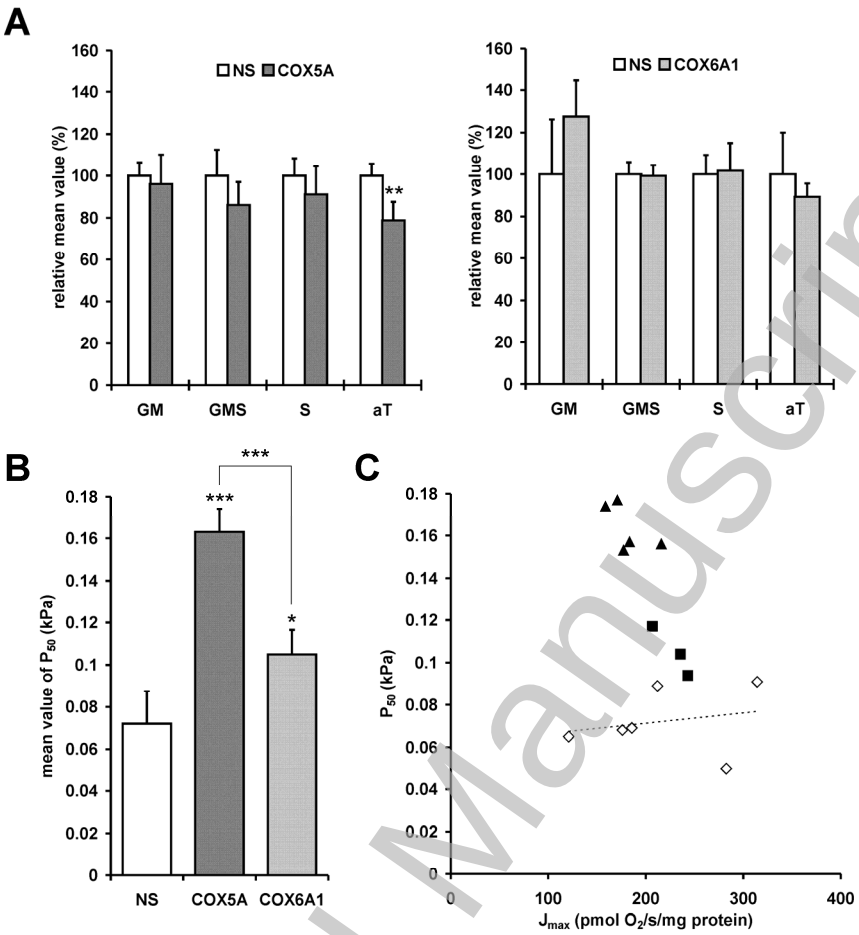

Figure 5

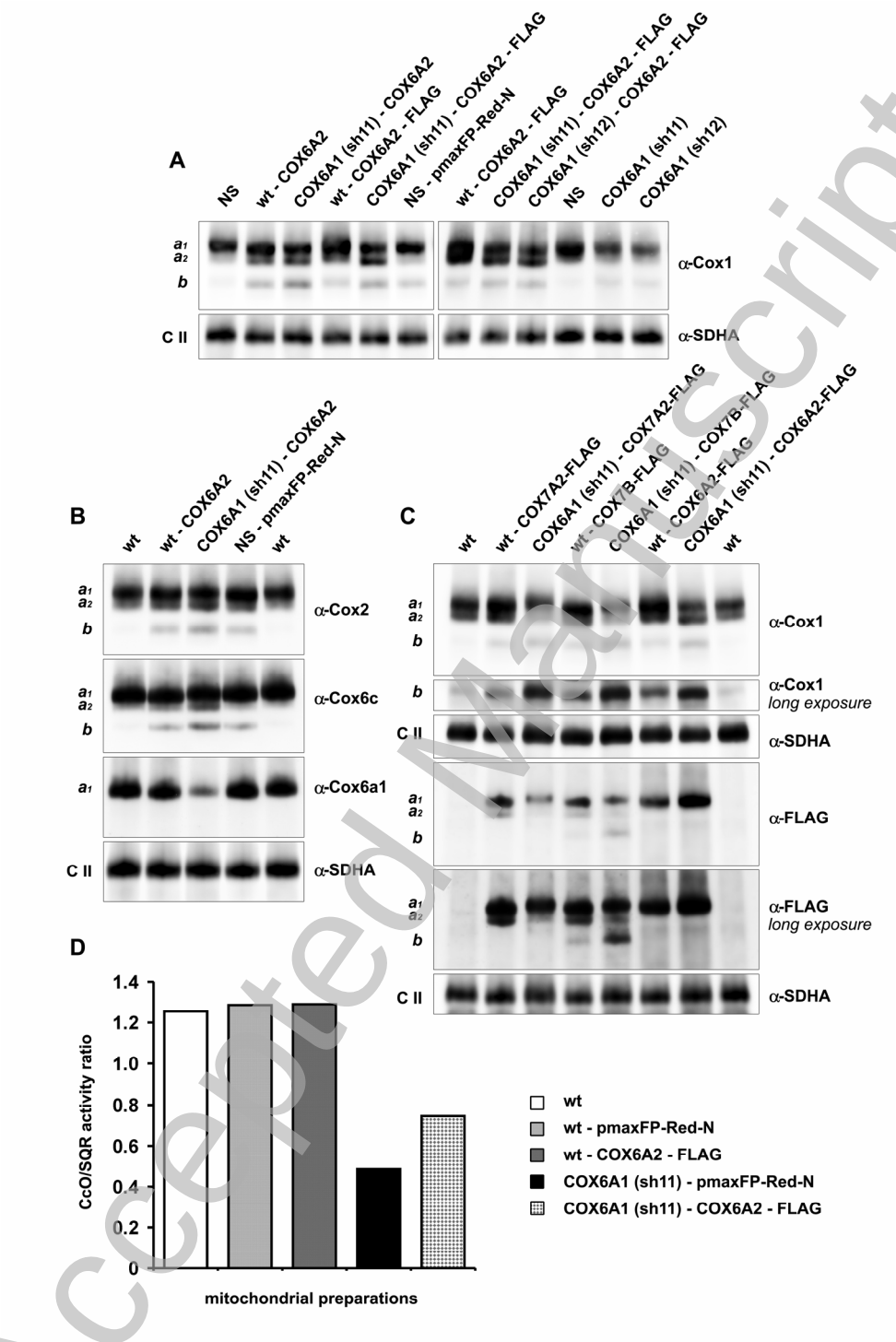

Scheme 1